

Electronic structure and energetics of pressure-induced two-dimensional C_{60} polymers

Susumu Okada

Institute of Material Science, University of Tsukuba, Tennodai, Tsukuba 305-8573, Japan

Susumu Saito

Department of Physics, Tokyo Institute of Technology 2-12-1 Oh-okayama, Meguro-ku, Tokyo 152-8551, Japan

(Received 5 August 1998)

We report on the electronic structure and energetic stabilities of two-dimensional C_{60} polymers, in both tetragonal and rhombohedral phases, studied by using the local-density approximation in the framework of the density-functional theory. Owing to hybrid networks of sp^2 -like (threefold coordinated) and sp^3 -like (fourfold coordinated) carbon atoms, the electronic structure of these phases is considerably different from that of face-centered-cubic (fcc) C_{60} . Both systems are found to be elemental semiconductors having small indirect gaps. Furthermore, since the interlayer distance between adjacent polymerized planes for both phases is small, these systems are found to have three-dimensional electronic structures. From structural optimizations under the experimental lattice parameters, we reveal energetic high stabilities of these phases. In particular, the tetragonal phase is found to be considerably more stable in energy than the fcc phase. Its high stability is caused by the formation of intercluster bonds whose energy gain is larger than the energy loss due to the distortion of the carbon networks of C_{60} units upon polymerization. [S0163-1829(99)04603-2]

I. INTRODUCTION

Following the macroscopic production of C_{60} and other fullerenes, there have been many experimental and theoretical studies on this form of carbon.¹⁻³ Although C_{60} and other fullerenes consist of sp^2 carbon atoms, fullerenes have a zero-dimensional C-C network which is different from diamond (three-dimensional network) and graphite (two-dimensional network). This is the reason why fullerenes are classified as a form of carbon. Since fullerenes have a moderate chemical reactivity, various new carbon network materials derived from fullerenes have been synthesized and studied intensively.⁴⁻⁷ In the case of solid C_{60} phases, C_{60} clusters behave as weakly interacting spheres and play an atomlike role to form a face-centered-cubic (fcc) lattice. The electronic structure of the solid C_{60} is different from that of metallic graphite and insulating diamond.⁸ The band structure of solid C_{60} is semiconducting, and corresponds to the electronic structure of the C_{60} cluster.⁸ Hence the cohesive mechanism between the clusters is considered to be via van der Waals interaction.

In the last five years, several crystalline phases possessing two- or one-dimensional infinite carbon networks have been synthesized from solid C_{60} .⁹⁻¹³ This family of crystalline phases is called fullerene polymers or C_{60} polymers. In contrast to the fcc C_{60} phase, C_{60} polymers have covalent bonds between adjacent clusters. The existence of intercluster bonds causes the distortion of C_{60} clusters from a truncated icosahedron which may induce drastic changes of physical properties of the system. First, Rao *et al.* reported the polymerization of C_{60} by exposing solid C_{60} to light.⁹ However, their structure has not yet been identified. On the other hand, at room temperatures or lower, AC_{60} ($A = K, Rb, \text{ or } Cs$) is found to form a one-dimensionally polymerized phase (orthorhombic phase) in which polymerization is generated along the (110) direction of the fcc lattice.¹⁰ In addition, an

external pressure applied to solid C_{60} at high temperatures has been found to induce polymerization of C_{60} to give three distinct phases (orthorhombic, tetragonal, and rhombohedral phases).¹¹⁻¹³ These crystalline phases of pristine C_{60} polymers have been identified by several experimental procedures so far. It should be mentioned that the polymerization is attained via formation of the four-membered ring or [2+2] cycloaddition of "66" bonds, which is the adjoining edge between two six-membered rings in C_{60} . Although the obtained orthorhombic phase is formed by a C_{60} -based one-dimensional chain similar to that of A_1C_{60} ,¹⁰ rhombohedral and tetragonal phases were found to have two-dimensionally polymerized layers in which the C_{60} clusters form triangular and square lattice respectively (Fig. 1). These phases can be classified as a form of crystalline carbon consisting of both sp^2 -like (threefold coordinated) and sp^3 -like (fourfold coordinated) C atoms.¹⁴⁻¹⁶ A characteristic of this synthetic procedure is that one can control the obtained polymerized phases by tuning the pressure and temperature.^{17,18} The orthorhombic phase is synthesized in a lower-temperature region. On the other hand, the two-dimensionally polymerized phases are obtained under high-temperature conditions. Among two-dimensional C_{60} polymers, the rhombohedral phase is found to be the majority phase, and the tetragonal phase appears only as a subphase in the lower pressure region.

In a previous paper, we reported on the electronic structure of the rhombohedral phase obtained by using density-functional theory.¹⁹ In the present paper we report on the electronic structure of the tetragonal phase including the effect of the stacking structure, and this is compared to that of the rhombohedral phase. Since the systems attract much interest not only as crystalline carbon systems but also host materials for various kinds of intercalants,²⁰ it should be important to study their energetic stabilities as well as their electronic structure. In order to reveal the electronic struc-

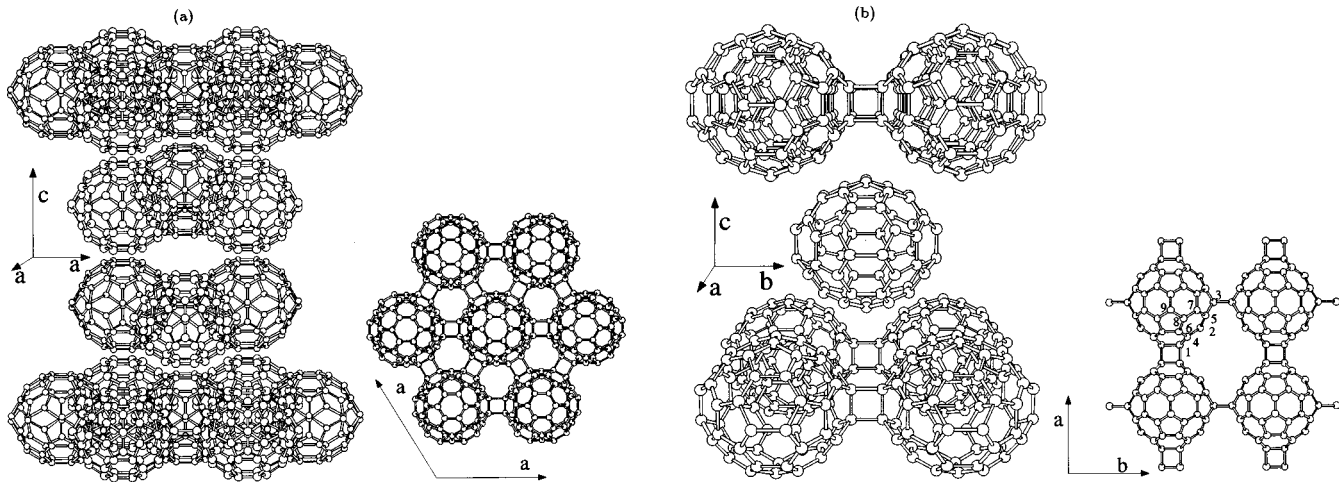


FIG. 1. Geometric structure of two-dimensional C_{60} polymer phases. (a) Rhombohedral phase (b) tetragonal phase.

ture, we use density-functional theory under the geometries giving an excellent agreement with the x-ray-diffraction pattern reported by Núñez-Regueiro *et al.*¹² and Xu and Scuseria²¹. Next, we perform the geometry optimization for these phases under observed lattice parameters, and discuss the detailed energetics of these layered solid carbon systems.

This paper is organized as follows. In Sec. II, the computational method used in this work is given. Results and discussions are given in Sec. III. We conclude the paper in Sec. IV.

II. COMPUTATIONAL METHODS

In the present work, the electronic and geometric structures have been studied by using the local-density approximation (LDA) in the density-functional theory.^{22,23} To express the exchange-correlation potential of electrons, we use a functional form fitted to the Ceperley-Alder result.^{24,25} A norm-conserving pseudopotential generated by using the Troullier-Martins scheme is adopted to describe the electron-ion interaction.²⁶ In constructing the pseudopotential, the core radii adopted for C $2s$ and $2p$ states are both 1.5 bohr. The valence wave functions are expanded by plane-wave basis sets with a cutoff energy of 50 Ry, which gives enough convergence of the total energy to discuss the relative stability of various carbon phases.^{26,27} We adopt the conjugate-gradient procedure both for the self-consistent electronic-structure calculation and geometric optimization.²⁸ Furthermore, we use the supercell procedure for total-energy calculations of single sheets of polymerized C_{60} and isolated C_{60} units, with the distortion formed in the rhombohedral and tetragonal phases.

III. RESULTS AND DISCUSSIONS

A. Electronic structure

The geometric structure of the rhombohedral phase is shown in Fig. 1(a). C_{60} clusters form a triangular lattice in each layer, and these layers are stacked along the c -axis direction in $ABCABC \dots$ order. The space group of the system is $R\bar{3}m$. Owing to the polymerization, each C_{60} cluster

is distorted from I_h symmetry and connected to adjacent clusters via 12 sp^3 -like carbons. Hence, the system possesses 48 sp^2 -like and 12 sp^3 -like carbon atoms. The lattice parameters observed in the experiment are $a=9.19 \text{ \AA}$ and $c=24.5 \text{ \AA}$ in the hexagonal representation. Then the inter-layer distance is $c/3$.

The electronic band structure of the rhombohedral phase is shown in Fig. 2. There are several important features in the band structure different from these of the fcc C_{60} phase. A fundamental gap between the top of the valence band (Z point) and the bottom of the conduction band (F point) is found to be 0.35 eV. This value is considerably smaller than that of the fcc C_{60} phase (1.06 eV) obtained by using the same computational procedure. Furthermore, the value does not approach that of diamond, in spite of the presence of the 12 sp^3 -like atoms. Although the LDA generally underestimates the energy gap between these band extremes, the difference between the band gaps of the rhombohedral and fcc phases should be reliable. It is well known that each energy band of the fcc C_{60} phase corresponds with one of the energy levels of the C_{60} molecule. However, in the case of the rhombohedral phase, the band structure of the phase is considerably different from that of the fcc phase and we cannot observe such a correspondence. The lowest branch of the conduction band of the rhombohedral phase is separated

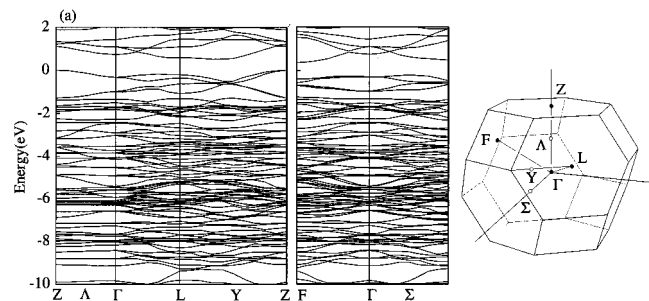


FIG. 2. Band structure of the two-dimensionally polymerized rhombohedral C_{60} . The energy is measured from the top of the valence band at the Z point. Symmetry points and lines in the first Brillouin zone of the rhombohedral lattice are also given (Ref. 19).

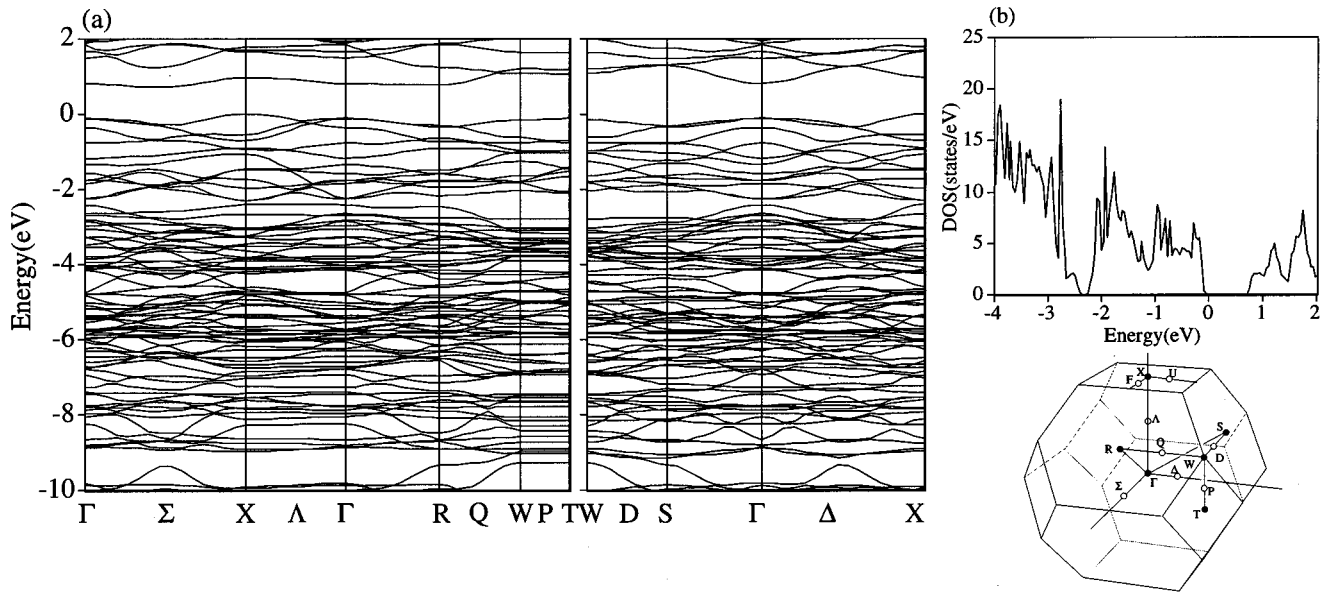


FIG. 3. (a) Band structure of the two-dimensionally polymerized tetragonal C_{60} . The energy is measured from the top of the valence band at the X point. (b) Density of states of tetragonal C_{60} . Symmetry points and lines in the first Brillouin zone of the orthorhombic body-centered lattice are also given.

from higher conduction-band states. In addition, band dispersions are larger than those of the fcc phase. In particular, a large band dispersion is observed in a deep valence-band region corresponding to σ -electron states, and is caused mainly by the formation of intercluster bonds.

Although the system has a stacking two-dimensional structure, a rather large band dispersion along the Λ line shows that the system is electronically three dimensional. In fact, inverse effective mass tensor values for directions parallel and perpendicular to the polymerization plane are of the same order for both holes and electrons. The effective masses at the bottom of the conduction band (electron masses) obtained by the diagonalization of the tensor are $0.2m_e$, $0.7m_e$, and $0.9m_e$ (m_e is the bare electron mass). On the other hand, the effective masses at the top of the valence band (hole masses) are $0.5m_e$, $0.6m_e$, and $1.8m_e$.

We now pay attention to the other two-dimensional C_{60} polymer phase, i.e., the tetragonal phase. As shown in Fig. 1(b), C_{60} clusters form a square lattice in each layer, and the space group of this system is $Immm$ (body-centered-orthorhombic). However, the lattice parameters are $a=b=9.09 \text{ \AA}$ and $c=14.95 \text{ \AA}$, and this phase is called the "tetragonal phase" owing to the equivalence of a and b values. The electronic structure obtained for this phase is also considerably different from that of the fcc phase.

In Fig. 3(a), the energy-band structure of the tetragonal-phase C_{60} polymer is shown. The top of the valence band is found to be at the X point, and the bottom of the conduction band is on the Σ line. The fundamental energy gap between these band extremes is 0.72 eV . This value is larger than that of the rhombohedral phase but smaller than that of the fcc C_{60} phase. The rather separated lowest branch of the conduction band is also observed in this phase as in the case of the rhombohedral phase.¹⁹ Furthermore, since the valence-band

structure is considerably different from that of the fcc phase, each band of the phase does not correspond with that of the fcc phase.

The characteristics observed in the lower conduction band and the higher valence band must depend on the network topology of π -electron systems. In the case of the rhombohedral phase, only 48 C atoms out of 60 atoms in each C_{60} possess the π state. In addition, these atoms are divided into two equivalent 24-atom groups above and below the polymerized plane [Fig 4(a)]. Hence the π -electron states of the phase are regarded like those of the C_{24} cluster which forms a triangular lattice above (below) the polymerized plane. A similar interpretation is considered for the tetragonal phase. In the case of a tetragonal C_{60} polymer, 52 C atoms possess π states in each C_{60} . Therefore, the constituent unit of this system concerning π states is found to be a hollow-cage C_{52} having D_{2h} symmetry [Fig. 4(b)]. Hence it is natural that the band structure around the fundamental gap in the rhombohedral and tetragonal phases is different from that of the fcc phase.

A band dispersion is generally larger than that of the fcc C_{60} , and all the unoccupied states form one continuous con-

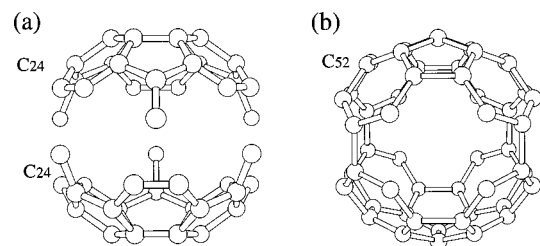


FIG. 4. Schematic geometric structure of π -electron systems. (a) The C_{24} bowl-shaped clusters forming a triangular lattice above and below polymerized planes in the rhombohedral phase. (b) C_{52} units forming a square lattice in the tetragonal phase.

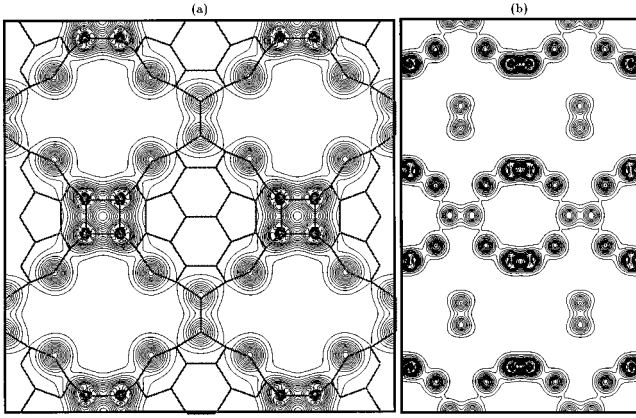


FIG. 5. Contour map of the valence-electron densities of the tetragonal C_{60} polymer on the (a) (001) and (b) (010) planes. The difference between each neighbor contour is 0.021 052 7 a.u. The projected C-C network on the (001) plane is also shown in (a), and the electron-density distribution corresponding to the C_4 rings with the intercluster bonds is apparent.

duction band. In particular, owing to the polymerization, a large band dispersion along Σ and Δ lines corresponding to polymerized directions is clearly observed in lower-energy states, i.e., in σ states. In addition, a rather clear band dispersion for π states along the Λ line shows that the tetragonal phase is electronically a three-dimensional system, as in the case of a rhombohedral phase. Effective masses at the bottom of the conduction band are $1.2m_e$, $0.4m_e$, and $1.1m_e$. Also the effective masses of the top of the valence band are $0.5m_e$, $0.5m_e$, and $0.8m_e$. From the density of states (DOS) obtained [Fig. 3(b)], we may be able to design several conducting materials with metal atoms doped into the interstitial sites, such as alkali or alkaline-earth metal-doped rhombohedral C_{60} polymers.²⁹

In Fig. 5, the valence-electron densities of the tetragonal phase are shown. It is evident that there is as much charge in *intercluster* C1-C1 bonds as in *intracluster* C1-C1 bonds. There are nine inequivalent atoms in the tetragonal phase and are identified as C1–C9 in Fig. 1(b). The electron density clearly indicates that carbon atoms connecting adjacent clusters are actually fourfold-coordinated atoms as in the case of diamond. However, bond angles associated with these fourfold-coordinated atoms are considerably different from

TABLE I. Optimized atomic coordinations of the tetragonal phase under the reported lattice parameters. Atomic indices are given in Fig. 1(b).

C1	0.41215	0.08838	0.00000
C2	0.24971	0.28357	0.04853
C3	0.00000	0.41288	0.05256
C4	0.33217	0.15912	0.07715
C5	0.12836	0.33410	0.09479
C6	0.28343	0.08007	0.14952
C7	0.07895	0.25117	0.16837
C8	0.15511	0.12707	0.19583
C9	0.07586	0.00000	0.22438

the ideal sp^3 hybridization angle of 109.47° . Bond angles of the sp^3 -like atoms, under the fully optimized geometry (Table I) to be mentioned in detail in Sec. III B, are $\theta_{C_4C_1C_1'} = 118.84^\circ$, $\theta_{C_4C_1C_4} = 99.84^\circ$, $\theta_{C_4C_1C_1} = 115.25^\circ$, $\theta_{C_1C_1C_1'} = 90.00^\circ$, $\theta_{C_5C_3C_3'} = 118.36^\circ$, $\theta_{C_5C_3C_3} = 114.76^\circ$, $\theta_{C_3C_3C_3'} = 90.00^\circ$, and $\theta_{C_5C_3C_5} = 101.42^\circ$, where C1' and C3' are the C1 and C3 atoms in the adjacent cluster [Fig. 1(b)]. Since we assume a D_{2h} symmetry for this calculation, $\theta_{C_1C_1C_1'}$ and $\theta_{C_3C_3C_3'}$ must be 90.00° . The strength of these intercluster bonds (C1-C1 and C3-C3) estimated as the energy gain upon the bond formation by using the Tersoff potential,^{30,31} is about 1.5 eV per bond, which is smaller than that of the ideal value for diamond by about 2.1 eV per bond. Such sp^3 -like carbon atoms also exist in the rhombohedral phase. In sharp contrast to the above intercluster interaction within a polymerized layer, there is no sizable charge density in an interlayer region. Hence the cohesion between layers of two-dimensional C_{60} polymers is considered to be via a van der Waals interaction similar to that of graphite.

Next we consider the effect of the stacking disorder to two-dimensional (100) planes mentioned by Nunez-Regueiro *et al.*¹² under the reported lattice parameters ($a=b=9.09$ Å). We calculate the DOS by using the generalized tight-binding (TB) model³² to estimate the effect of the stacking difference. Since the TB model used in the present works takes account of not only the transfer but also the overlap matrix elements, the band structure of bonding σ states, bonding π states, and antibonding π states are expected to be reliable.³³ In Fig. 6, we show DOS's for two

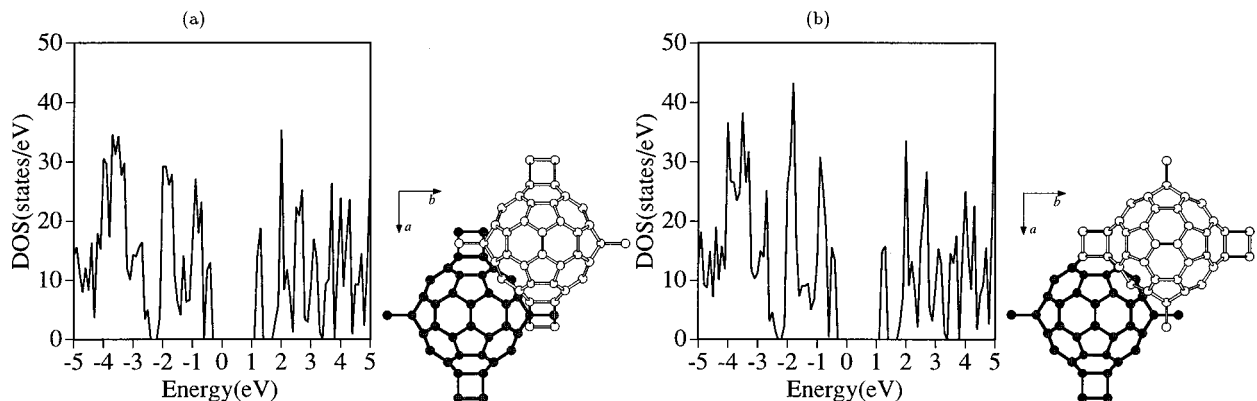


FIG. 6. (a) DOS of the “tetragonal” (orthorhombic) AAAA... stacking structure, and (b) the DOS of the tetragonal ABAB... stacking structure obtained by using the generalized tight-binding model.

TABLE II. Total energies per atom of fcc C_{60} , the polymerized rhombohedral C_{60} , the polymerized tetragonal C_{60} , a single sheet of rhombohedral polymer (R sheet), a single sheet of tetragonal polymer (T sheet), a distorted C_{60} unit of the rhombohedral phase (R unit), and a distorted C_{60} unit of the tetragonal phase (T unit) obtained by the LDA. Energies are measured from the total energy of graphite. In the rhombohedral and tetragonal phases, as well as the fcc phase, geometries are fully optimized under the measured lattice constants. For the polymerized sheet and the distorted units calculations (R sheet, T sheet, R unit, and T unit), atoms are fixed at the same position as in the geometries optimized under experimental lattice parameters, and the supercell calculation is adopted. In addition, the LDA total energies of rhombohedral and tetragonal phases under the initial geometries (Ref. 21) are also given.

	Total energy (eV)
R unit	0.6033
R sheet	0.4357
rhombohedral (optimized geometry)	0.4286
rhombohedral (initial geometry)	0.4407
T unit	0.5280
T sheet	0.4135
tetragonal (optimized geometry)	0.4059
tetragonal (initial geometry)	0.4226
fcc	0.4274

different stacking structures, i.e., ‘‘tetragonal’’ (orthorhombic symmetry) $AAAA \dots$ and tetragonal $ABAB \dots$ stacking structures. Although there is a little quantitative difference between two DOS’s, we can regard them as essentially the same DOS profile. Hence we can expect that characteristics of the electronic structure obtained by the LDA for the $AAAA \dots$ stacking in this work is also present in other stacking geometries.

B. Energetics

In this subsection, we study the structural parameters of the rhombohedral and tetragonal phases, and we also discuss the origin of the high stability found for the polymer phases. The structural optimization has been performed by using the conjugate-gradient method in the LDA under the experimentally reported lattice parameters, with a tight-binding geometry as an initial structure.^{12,21} Total energies per atom of the optimized geometries for these phases are listed in Table II together with those of the initial geometries and that of the fcc phase.

In the case of the rhombohedral phase, the difference between the energies of the optimized and initial geometries is very small. Furthermore, the relaxation from the initial geometry is also small. The diameter of a C_{60} unit along the c axis decreases by only 0.08 Å, while the extension along other axes are even smaller. The small reduction should be caused by the stacking effect. Furthermore, the total energy of the rhombohedral phase is found to be very close to that of the fcc phase, and their difference is only 0.001 eV per atom.

On the other hand, in the case of the tetragonal phase, the optimized atomic coordinates listed in Table I are rather dif-

ferent from these in the initial geometry. The geometrical relaxation obtained is the compression of the C_{60} unit along the c axis, and the extension along other axes similar to the rhombohedral phase. However, the extension along the a axis is smaller than that along the b axis. Intercluster C-C bond lengths both along the a axis, i.e., the C1-C1 bond, and along the b axis, i.e., the C3-C3 bond, are decreased compared with that of the initial geometry (1.64 Å). The optimized bond lengths are 1.597 Å for C1-C1 bonds and 1.584 Å for C3-C3 bonds.

As a result of this inequality in intercluster bond lengths, the lattice parameter values along a and b axes should be slightly different from one another as expected from the observed $Immm$ (orthorhombic) symmetry. Under the reported lattice parameters $a=b$, either the alternative stacking of 90°-rotated polymerized planes ($ABAB \dots$, the tetragonal stacking) or a stacking disorder of A and B planes is expected to be present in the tetragonal C_{60} polymer.

The total energy per atom for the optimized geometry of the tetragonal phase is listed in Table II. The total energy is found to be considerably lower than that of not only the rhombohedral phase but also the fcc phase. In order to examine the origin of the energetic high stability of the tetragonal phase, we first estimate the strength of the interlayer interaction (van der Waals interaction) E_{vdW}^{inter} . We also show the total energies of an isolated polymerized plane of the tetragonal phase (T sheet) together with that of the rhombohedral phase (R sheet) in Table II. In these calculations, we use a supercell procedure in which interlayer distances between adjacent layers are long enough to eliminate the interlayer interaction (12 and 10 Å for R and T sheets, respectively), and atoms in each layer are fixed to the optimized positions under the reported lattice parameters. The obtained energy value is 0.4134 eV, and the magnitude of the interlayer interaction is 0.008 eV. The total energy of the single tetragonal sheet itself is lower than that of the fcc C_{60} and rhombohedral phases. Hence the interlayer interaction is not the main origin of the high stability of the tetragonal phase. It should be noted that the interlayer interactions per C_{60} - C_{60} pair for both tetragonal and rhombohedral phases are close to each other (0.142 and 0.114 eV, respectively).

Furthermore, we also study the total energies of distorted C_{60} units disconnected from the adjacent clusters for both polymerized phases to calculate the energy gain due to the formation of intercluster bonds (Table II). The total energy of the distorted C_{60} unit of the tetragonal phase obtained by using the supercell procedure in the LDA is found to be lower than that of the distorted unit of the rhombohedral phase. On the other hand, since eight and 12 intercluster bonds exist in the tetragonal and rhombohedral phases respectively, the energy gain due to polymerization in the tetragonal phase should be smaller than that in the rhombohedral phase. In order to estimate of the energy gain per intercluster bond, we consider the total energy of the system to be the sum of following four terms:

$$E_{tot} = E_{unit} + E_{vdW}^{inter} + E_{vdW}^{intra} + E_{C-C},$$

where E_{unit} , E_{vdW}^{inter} , E_{vdW}^{intra} , and E_{C-C} are the total energy of the distorted C_{60} unit, the *interlayer* van der Waals interaction energy as mentioned above, the *intralayer* van der

Waals interaction energy, and intercluster C-C bond formation energy, respectively. Since the LDA can give only the sum of E_{vdW}^{intra} and E_{C-C} , we assume E_{vdW}^{intra} to be equal to the average of E_{vdW}^{inter} for both phases (0.13 eV). Roughly estimated values of the energy gain upon the intercluster-bond formations in this way is about 1.6 eV per bond in both rhombohedral and tetragonal phases. Hence we can conclude that intercluster bonds play an important role in stabilizing the phases. In addition, the energetic stability of the distorted C_{60} unit is also important. In particular, the remarkably high stability of the tetragonal phase is attributed to the rather small distortion of the C_{60} unit.

IV. CONCLUSION

In this paper, we studied the electronic and geometric structures of rhombohedral and tetragonal phases of two-dimensional C_{60} polymers by using the local-density approximation. Owing to short C_{60} - C_{60} distances both within and between layers, rhombohedral and tetragonal phases were found to be electronically three dimensional, and to be elemental semiconductors having indirect gaps. The band structure of these phases do not correspond to that of the fcc phase, on to the energy levels of the C_{60} cluster. Hence we can classify these phases as new crystalline carbon systems not only by their network geometries but also due to their electronic structure. The total energy of the rhombohedral phase was found to be very close to that of the fcc phase. More surprisingly, the tetragonal phase is the most stable phase among these phases, i.e., fcc, rhombohedral, and tetragonal phases, although the tetragonal phase is usually a minority phase in pressure-polymerized solid C_{60} . In addition, we obtained the magnitude of the interlayer-interaction

energy not only for the tetragonal phase but also for the rhombohedral phase. It was revealed that interlayer interaction plays an important role in stabilizing both rhombohedral and tetragonal phases. However, the interlayer interaction is not the main origin of the remarkable stability of the tetragonal phase. Instead, the small distortion of the C_{60} unit and the formation of the intercluster bond should be the origins of its high stability.

The present study suggests that, by controlling the number of intercluster bonds (sp^3 -like C atoms) in polymerized fullerenes, we would be able to produce various kinds of hybrid carbon network materials of sp^2 and sp^3 C atoms, the electronic structure of which are different from that of previously synthesized C-C networks. Furthermore, owing to their layered structures, we would also be able to design intercalation compounds having notable properties based on polymerized C_{60} as a host material.

ACKNOWLEDGMENTS

We would like to thank Professor A. Oshiyama, Dr. M. Saito, Dr. O. Sugino, Dr. Y. Miyamoto, Professor N. Hamada, and Professor S. Sawada for providing the program used in this work. We also would like to thank Professor Y. Iwasa for fruitful discussions. Numerical calculations were performed on the Fujitsu VPP500 computer at Institute for Solid State Physics, University of Tokyo and the NEC SX3/34R, and the HPC computer at Institute for Molecular Science, Okazaki National Institute. This work was supported by The Japan Society for the Promotion of Science under Contract No. RFTF96P00203 and The Nissan Science Foundation. S. O. was supported by the JSPS.

¹W. Krätschmer, L. D. Lamb, K. Fostiropoulous, and D. R. Hoffman, *Nature (London)* **347**, 354 (1990).

²K. Kikuchi, N. Nakahara, T. Wakabayashi, S. Suzuki, H. Shiro-maru, Y. Miyake, K. Saito, I. Ikemoto, M. Kainosho, and Y. Achiba, *Nature (London)* **357**, 142 (1992).

³Y. Achiba, K. Kikuchi, Y. Aihara, T. Wakabayashi, Y. Miyake, and M. Kainosho, in *Science and Technology of Fullerene Materials*, edited by P. Bernier, T. W. Ebbesen, D. S. Bethune, R. M. Metzger, L. Y. Chiang, and J. W. Mintmine *et al.* (MRS Symposia Proceedings No. 359 (Materials Research Society, Pittsburgh, 1995), p. 3.

⁴A. F. Hebard, M. J. Rosseinsky, R. C. Haddon, D. W. Murphy, S. H. Glarum, T. T. M. Palstra, A. P. Ramirez, and A. R. Kortan, *Nature (London)* **350**, 632 (1991).

⁵M. J. Rosseinsky, A. P. Ramirez, S. H. Glarum, D. W. Murphy, R. C. Haddon, A. F. Hebard, T. T. M. Palstra, A. R. Kortan, S. M. Zahurak, and A. V. Makhija, *Phys. Rev. Lett.* **66**, 2830 (1991).

⁶P. W. Stephens, L. Mihaly, P. L. Lee, R. L. Whetten, S. Huang, R. Kaner, F. Deiderich; and K. Holzer, *Nature (London)* **351**, 632 (1991).

⁷K. Tanigaki, T. W. Ebbesen, S. Saito, J. Mizuki, J. S. Tsai, Y. Kubo, and S. Kuroshima, *Nature (London)* **352**, 222 (1991).

⁸S. Saito and A. Oshiyama, *Phys. Rev. Lett.* **66**, 2637 (1991).

⁹A. M. Rao, P. Zhou, K. Wang, G. T. Hager, J. M. Holden, Y.

Wang, W. Lee, X. Bi, P. C. Eklund, D. S. Cornett, M. A. Duncan, and I. J. Amster, *Science* **259**, 955 (1993).

¹⁰O. Chauvet, G. Oszlanyi, L. Forro, P. W. Stephens, M. Tegze, G. Faigel, and A. Janossy, *Phys. Rev. Lett.* **72**, 2721 (1994).

¹¹Y. Iwasa, T. Arima, R. M. Fleming, T. Siegrist, O. Zhou, R. C. Haddon, L. J. Rothberg, K. B. Lyons, H. L. Carter Jr., A. F. Hebard, R. Tycko, G. Debbagh, J. J. Krajewski, G. A. Thomas, and T. Yagi, *Science* **264**, 1570 (1995).

¹²M. Núñez-Regueiro, L. Marques, J.-L. Hodeau, O. Béthoux, and M. Perroux, *Phys. Rev. Lett.* **74**, 278 (1995).

¹³G. Oszlanyi and L. Forro, *Solid State Commun.* **93**, 265 (1995).

¹⁴C. Goze, F. Rachidi, M. Núñez-Regueiro, L. Marques, J.-L. Hodeau, and M. Mehring, *Phys. Rev. B* **54**, R3676 (1996).

¹⁵Y. Maniwa, M. Sato, K. Kume, M. E. Kozlov, and M. Tokumoto, *Carbon* **34**, 1207 (1996).

¹⁶A. M. Rao, P. C. Eklund, J.-L. Hodeau, L. Marques, and M. Núñez-Regueiro, *Phys. Rev. B* **55**, 4766 (1998).

¹⁷Y. Iwasa, *Solid State Phys. (Tokyo)* **31**, 909 (1996) (in Japanese).

¹⁸L. Marques, J.-L. Hodeau, M. Núñez-Regueiro, and M. Perroux, *Phys. Rev. B* **54**, R12 633 (1996).

¹⁹S. Okada and S. Saito, *Phys. Rev. B* **55**, 4039 (1997).

²⁰T. Furudate, Y. Iwasa, T. Mitani, T. Arima, and T. Yagi, in *Abstracts of the 51st Annual Meeting of the Physical Society of Japan (Kanazawa, 1996)* (Physical Society of Japan, Tokyo, 1996), Pt. 2, p. 357.

- ²¹C. H. Xu and G. E. Scuseria, Phys. Rev. Lett. **74**, 274 (1995).
²²P. Hohenberg and W. Kohn, Phys. Rev. B **136**, 864 (1964).
²³W. Kohn and L. J. Sham, Phys. Rev. A **140**, 1133 (1965).
²⁴D. M. Ceperley and B. J. Alder, Phys. Rev. Lett. **45**, 566 (1980).
²⁵J. P. Perdew and A. Zunger, Phys. Rev. B **23**, 5048 (1981).
²⁶N. Troullier and J. L. Martins, Phys. Rev. B **43**, 1993 (1991).
²⁷L. Kleinman and D. M. Bylander, Phys. Rev. Lett. **48**, 1425 (1982).
²⁸O. Sugino and A. Oshiyama, Phys. Rev. Lett. **68**, 1858 (1992).
²⁹S. Okada and S. Saito (unpublished).
³⁰J. Tersoff, Phys. Rev. Lett. **61**, 2879 (1988).
³¹J. Tersoff, Phys. Rev. B **37**, 6991 (1988).
³²N. Hamada and S. Sawada (unpublished).
³³S. Okada, Ph.D thesis, Department of Physics, Tokyo Institute of Technology, 1998.